On Constructing an Explicit Algebraic Stress Model Without Wall-Damping Function

Noma Park and Jung Yul Yoo*

School of Mechanical and Aerospace Engineering, Seoul National University, Seoul 151-742, Korea

In the present study, an explicit algebraic stress model is shown to be the exact tensor representation of algebraic stress model by directly solving a set of algebraic equations without resort to tensor representation theory. This repeals the constraints on the Reynolds stress, which are based on the principle of material frame indifference and positive semi-definiteness. An a priori test of the explicit algebraic stress model is carried out by using the DNS database for a fully developed channel flow at $Re_\tau=135$. It is confirmed that two-point correlation function between the velocity fluctuation and the Laplacians of the pressure-gradient i s anisotropic and asymmetric in the wall-normal direction. Thus, a novel composite algebraic Reynolds stress model is proposed and applied to the channel flow calculation, which incorporates non-local effect in the algebraic framework to predict near-wall behavior correctly.

Key Words : Explicit Algebraic Reynolds Stress Model, Tensor Representation Theory, Elliptic Relaxation Model, Near-Wall Limiting Behaviour, Channel Flow

Nomenclature

b_{ij}, $\boldsymbol{b}$: Reynolds stress anisotropy, $\dfrac{\overline{u_iu_j}-\frac{2}{3}k\delta_{ij}}{2k}$

C_μ : Coefficient in linear and nonlinear eddy viscosity models, Eqs. (6) and (16)

C_i : Coefficients in pressure-strain models, $i=1, 2, 3, 4$

C_T : Coefficient of Kolmogorov time scale, Eq. (12)

$C_{\varepsilon 1}, C_{\varepsilon 2}$: Coefficients in ε-equation

C_{Lij} : Coefficients in correlation length scale components, Eq. (31)

$C_{\eta ij}$: Coefficients in Kolmogorov length scale components, Eq. (31)

D_{ij} : Turbulent transport term+viscous diffusion term, $T_{ij}+\nu\nabla^2\overline{u_iu_j}$

D_k : Transport+diffusion in the turbulent kinetic energy equation, $\frac{1}{2}D_{ii}$

D/Dt : Derivative following the mean flow, $\dfrac{\partial}{\partial t}+U_j\dfrac{\partial}{\partial x_j}$

k : Turbulent kinetic energy, $\frac{1}{2}\overline{u_iu_i}$

L : Correlation length scale for elliptic relaxation model

L_{ij} : Correlation length scale tensor in asymmetric elliptic model, Eq. (30)

P : Rate of production of turbulent kinetic energy, $\frac{1}{2}P_{ii}$

P_{ij} : Rate of production of Reynolds stress, $-\overline{u_iu_k}\dfrac{\partial U_j}{\partial x_k}-\overline{u_ju_k}\dfrac{\partial U_i}{\partial x_k}$

p : Hydrodynamic pressure

Re_τ : Reynolds number based on friction velocity and channel half width, $\dfrac{u_\tau\delta}{\nu}$

S_{ij}, S : Mean strain rate tensor, $\dfrac{1}{2}\left(\dfrac{\partial U_i}{\partial x_j}+\dfrac{\partial U_j}{\partial x_i}\right)$

T : New turbulence time scale, Eq. (12)

* Corresponding Author,
E-mail : jyyoo@plaza.snu.ac.kr
TEL : +82-2-880-7112; **FAX** : +82-2-883-0179
School of Mechanical and Aerospace Engineering, Seoul National University, San 56-1, Shinlim-dong, Kwanak-ku, Seoul 151-742, Korea. (Manuscript **Received** March 14, 2002; **Revised** August 9, 2002)

T_{ij} : Turbulent transport term, $-\frac{\partial}{\partial x_k}(\overline{u_i u_j u_k}+\overline{pu_i}\delta_{jk}+\overline{pu_j}\delta_{ik})$

U_i : Mean velocity components, (U, V, W)

u_i : Fluctuating velocity components, (u, v, w)

$\overline{u_i u_j}$: Reynolds stress components

W_{ij} $\boldsymbol{W}$: Mean rotation rate tensor, $\frac{1}{2}\left(\frac{\partial U_i}{\partial x_j}-\frac{\partial U_j}{\partial x_i}\right)$

x_i : Cartesian coordinates, (x, y, z)

$\boldsymbol{x}'-\boldsymbol{x}$: Separation vector in two-point correlations, Eqs. (18) and (19)

y^+ : Dimensionless wall normal distance, $\frac{u_\tau y}{\nu}$

Greek symbols

α : Coefficient in dissipation rate anisotropy model, Eq. (23)

δ : Channel half width

δ_{ij}, $\boldsymbol{I}$: Kronecker delta

ε_{ij} : Rate of dissipation of Reynolds stress, $2\nu\overline{\left(\frac{\partial u_i}{\partial x_k}\frac{\partial u_j}{\partial x_k}\right)}$

ε : Rate of dissipation of turbulent kinetic energy, $\frac{1}{2}\varepsilon_{ii}$

Φ_{ij} : Pressure-strain correlation, $\overline{p\left(\frac{\partial u_i}{\partial x_j}+\frac{\partial u_j}{\partial x_i}\right)}$

ϕ_{ij} : Velocity-pressure correlation, or redistributive term, $\frac{1}{\rho}\left(\overline{u_i\frac{\partial p}{\partial x_j}}+\overline{u_j\frac{\partial p}{\partial x_i}}\right)$

ν, ν_T : Molecular viscosity and eddy viscosity

II_{ij}, $\boldsymbol{II}$: Traceless redistribution tensor, $\phi_{ij-D}\varepsilon_{ij}$

ρ : Fluid density

σ : Amplitude of strain rate, $\sqrt{S_{nm}S_{mn}}$

σ_k, σ_ε : Coefficients in k-ε model, Eqs. (14) and (15)

τ : Large time scale of turbulence, $\frac{k}{\varepsilon}$

Subscripts

$_D(\ )_{ij}$: Deviatoric tensor operator, $(\ )_{ij}-\frac{1}{3}(\ )_{kk}\delta_{ij}$

Superscripts

DNS : DNS data

$\overline{(\ )}$: Reynolds-averaged value

$(\ )^+$: Wall unit, $\frac{u_\tau(\ )}{\nu}$

$(\ )^*$: Non-dimensional quantities introduced by Gatski & Speziale (1993), Eq. (6)

h : Homogeneous solution of PDE, Eqs. (21) and (22)

Symbols

$\|\cdot\|$: Vector norm

II_ϕ : Second invariant of a generic tensor ϕ_{ij}, $\phi_{ij}\phi_{ji}$

III_ϕ : third invariant of a generic tensor ϕ_{ij}, $\phi_{ij}\phi_{jk}\phi_{ki}$

1. Introduction

Since the earliest stage of turbulence modeling, it is believed that one-point correlations of velocity fluctuation components, or the Reynolds stress tensor, can be simply modeled in terms of the mean-velocity gradient and some dimensional scalars which describe scales of turbulent flows. The k-ε model based on simple eddy viscosity assumption is the first name that appears in the hierarchy of this kind of models. Another approach is to solve all the transport equations for the Reynolds stress components.

Although it has been long since Launder et al. (1975) closed second-order moment equations, this approach has not been adopted as a major engineering tool in predicting complex flows, since it is too tough to solve five additional transport equations for the Reynolds stress closure, which do not necessarily give exact solutions even for simple flows. Rodi (1976) proposed an assumption using local equilibrium hypothesis which yields a set of algebraic equations for the Reynolds stress tensor, say "Algebraic (Reynolds) Stress Model (ASM)". However, inversion of a 6×6 matrix at every grid point and every time step is by no means cheaper than solving full transport equations. Pope (1975) and Gatski & Speziale (1993) showed that an exact explicit solution of ASM can be obtained by using tensor representation theory. This approach was entitled "Explicit Algebraic Stress Model

(EASM)" and is regarded as a systematic and unified approach between nonlinear eddy viscosity model (NLEVM) and ASM. However, Wang (1997) (abbreviated as W97 hereinafter), criticized it in the light of the principle of material frame indifference (PMFI) and the positive semi-definiteness by showing that the Reynolds stress tensor can be influenced by the mean-velocity gradient only through the strain rate tensor.

In this study, the basic hypothesis of EASM, i.e., tensor representation theorem by Smith (1971), is reconsidered by comparing the results obtained by EASM with those obtained by a direct inversion of algebraic equations of ASM. Anyhow, some modification to the original model is inevitable for wall-bounded flow applications, because the model is totally invalid in the viscous sublayer. The linear model for the pressure-strain has no wall-reflection or viscous effects and the assumption of isotropic dissipation becomes untenable in the viscous sublayer. The extant low-Reynolds number modifications of EASM (Apsley & Leschziner, 1998; Wallin & Johanson, 2000) are made only in the empirical manner. They adopted damping functions in terms of wall distance and constants calibrated by curve-fitting to a specific DNS data. However, such a modification of the model is not pursued in this study obviously because little generality is expected to be obtained through such methodologies. An alternative approach is required to obtain a systematic low-Reynolds-number modification with sufficient generality. It is not a straightforward procedure to combine different time and length scales into a framework without damping functions. Readers may refer to Hanjalic (1994) and Wallin & Johanson (2000) and references cited therein for more comprehensive understanding of NLEVM, ASM and EASM. However, Durbin (1991) made it possible to integrate scale equations down to the wall without wall-damping functions by introducing new time and length scales in his k-ε-v^2 model at the cost of increased number of empirical constants, which are incorporated with an elliptic relaxation procedure to represent strongly non-homogeneous effects produced by the presence of the wall. The applicability of this novel concept to the algebraic stress model is investigated in this study.

On the other hand, the most annoying feature of developing and validating a turbulence model lies in full coupledness and nonlinear interaction between the mean and the turbulence equations. Therefore, some variables should be fixed, although simple substitution of the DNS data into algebraic formulas, as is used by most authors (for example, Mansour et al., 1988) gives no information on the mathematical and computational properties of a turbulence model. Parneix et al. (1998) introduced a new "differential a priori test", which consists in freezing some variables for which the DNS statistical fields are used and solving differential equations for the others. This approach enables one to construct a complete one-way coupling system for the equation of interest. A similar methodology using the DNS database is adopted in constructing a new ASM.

The objectives of this study are as follows:

1. To investigate the validity of the EASM, which will also provide a counter-example for PMFI and the proposal due to W97.
2. To verify the concept of elliptic relaxation procedure in the low-Reynolds number flow.
3. To propose a new composite EASM which incorporates inhomogeneous effect via the elliptic relaxation procedure.

This paper is organized as follows. First, EASM is outlined and the validity of the model is investigated, followed by some comments on the argument of W97. Next, some results on an a priori test for EASM and scale equations are presented. Then, closure models for non-homogeneous redistribution and dissipation rate anisotropy are introduced. In the penultimate section, a new composite algebraic stress model and its solution techniques are proposed including some illustrative calculation results. Finally, general conclusions and key findings are summarized in the last section.

2. Channel Flow Database

There are several works on the establishment of the DNS database (e.g., Kasagi et al., 1992; Moser et al., 1998), which supply complete statistics for a fully developed channel flow at various Reynolds numbers. However, an independent channel flow DNS is performed by the authors as some complicated statistics are required in this study such as two-point correlations of the velocity and the pressure gradient, which are not included in the available DNS database.

In the present channel flow DNS, $Re_\tau=135$ is chosen because this Reynolds number belongs to the lowest level of maintaining turbulence in which near-wall structure covers a large portion of the domain so that the flow can be a severe test case for high-Reynolds number models. The simulation code employed finite difference for spatial derivatives, and a semi-implicit scheme for time integration (Choi et al., 1993; Choi and Moin, 1994; Choi et al., 1994). The flow was computed on a grid of $97\times145\times145$ points in the streamwise (x), wall-normal (y), and spanwise (z) directions, respectively. The computational domain is of a $7\delta\times2\delta\times3.5\delta$ size in the x, y, and z directions, where δ denotes the channel half-width. This yields $\Delta x^+\approx10$ and $\Delta z^+\approx3.3$, which are sufficient enough to resolve most of the scales accurately. Although the simulation uses a 2nd-order central difference scheme on the staggered mesh, all spatial derivatives used in the post-processing of the data adopt 6th-order compact differences (Lele, 1992) in conjunction with 5th-order boundary closures in the wall-normal direction and weighted (filtered) 4th-order central differences (Vreman et al., 1996) in the homogeneous directions. This combination of difference schemes is chosen because it is free from odd-even decoupling, and thus prevents scattering of processed data while maintaining high accuracy. This property is important because successive differentiation is required to obtain higher order correlations and terms in each budget equation are directly utilized in constructing algebraic expressions for the Reynolds stresses. Figures 1

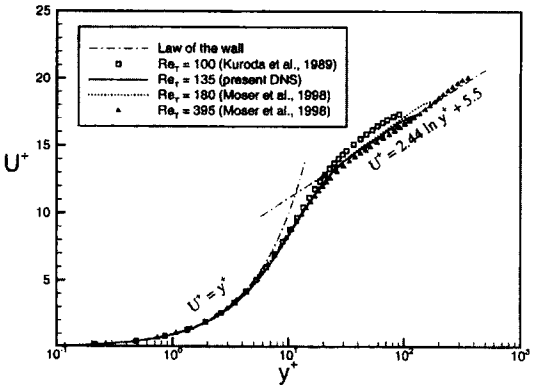

(a) Mean streamwise velocity

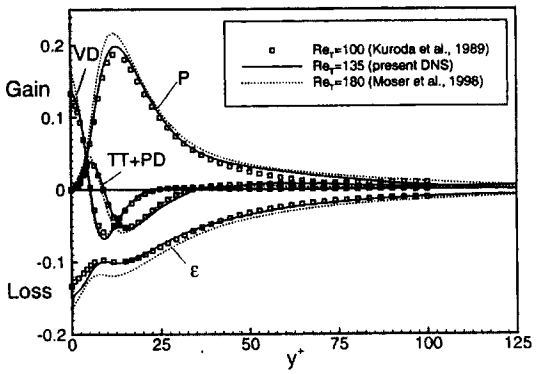

(b) Balances in the budget of turbulent kinetic energy; P=rate of production, ε=rate of dissipation, VD=viscous diffusion, TT=turbulent transport, PD=pressure diffusion

Fig. 1 Comparison and validation of the present channel flow DNS with other DNS results at comparable Reynolds numbers

(a) and 1(b) show mean streamwise velocity and balances in the budget of turbulent kinetic energy from the present DNS. Those from other DNS databases at Reynolds numbers of $Re_\tau=100$ (Kuroda et al., 1989; Kuroda, 1990), $Re_\tau=180$ and $Re_\tau=395$ (Moser et al., 1998) are also shown to check the adequacy of averaging field as well as the present DNS results. It is shown that the statistics from the present DNS are as accurate enough as those from other database.

3. Validation of EASM

In this section, the procedure of deriving EASM is outlined, based on the model of Gat-

ski & Speziale (1993, denoted as GS-EASM, hereinafter), followed by the validation of the model for the channel flow by directly comparing the solutions of EASM and ASM.

The Reynolds stress tensor is a solution of the transport equation :

$$\frac{D}{Dt}\overline{u_iu_j}=P_{ij}+D_{ij}+\Phi_{ij}-\varepsilon_{ij} \tag{1}$$

where P_{ij} denotes production, Φ_{ij} is the pressure-strain, ε_{ij} is the dissipation, and $D_{ij}=T_{ij}+\nu\nabla^2\overline{u_iu_j}$ is the turbulent transport plus the viscous diffusion. Note that the system rotation is not considered here for simplicity. Homogeneous turbulent flows in equilibrium, as well as regions of inhomogeneous turbulent flows, where there is a production-equal-to-dissipation equilibrium, satisfy the constraints :

$$\begin{aligned}\frac{D}{Dt}\overline{u_iu_j}-D_{ij}&\approx\frac{\overline{u_iu_j}}{k}\left(\frac{Dk}{Dt}-D_k\right)\\&=\frac{\overline{u_iu_j}}{k}(P-\varepsilon)\end{aligned} \tag{2}$$

Eq. (2), in conjunction with Eq. (1), leads to a set of algebraic equations for the Reynolds stress tensor :

$$\begin{aligned}(P-\varepsilon)\frac{\overline{u_iu_j}}{k}=&-\overline{u_iu_k}\frac{\partial U_j}{\partial x_k}-\overline{u_ju_k}\frac{\partial U_i}{\partial x_k}\\&+\Pi_{ij}-\frac{2}{3}\varepsilon\delta_{ij}\end{aligned} \tag{3}$$

Dissipation rate anisotropy models (Speziale and Gatski, 1997 ; Hallback et al., 1990) can also be incorporated in constructing Eq. (3), which will be discussed later. Rearranging Eq. (3) in terms of the strain rate tensor S_{ij} and the rotation rate tensor W_{ij} for the inertial frame, and the anisotropy tensor b_{ij} gives an alternate form :

$$\begin{aligned}(P-\varepsilon)b_{ij}=&-\frac{2}{3}kS_{ij}-k(b_{ik}S_{jk}+b_{jk}S_{ik}-\frac{2}{3}b_{mn}S_{mn}\delta_{ij})\\&+\frac{1}{2}\Pi_{ij}-k(b_{ik}W_{jk}+b_{jk}W_{ik})\end{aligned} \tag{4}$$

where the pressure-strain term including the deviatoric part of the dissipation remains as the only unclosed term. It is necessary that Π_{ij} should be a linear function of an anisotropic tensor to make Eq. (4) an algebraic set. Therefore, only linear models can be incorporated to realize this, which is one of the main drawbacks of ASM. The model of Launder et al. (1975, denoted as LRR, hereinafter) or Speziale et al. (1991, SSG) may be the possible candidate, which is given by

$$\begin{aligned}\Pi_{ij}=&-C_1\varepsilon b_{ij}+C_2kS_{ij}\\&+C_3k\left(b_{ik}S_{jk}+b_{jk}S_{ik}-\frac{2}{3}b_{mn}S_{mn}\delta_{ij}\right)\\&+C_4k(b_{ik}W_{jk}+b_{jk}W_{ik})\end{aligned} \tag{5}$$

where model coefficients C_i are either constants or functions of nondimensional scalars such as Π_b, which are listed in Table 1 for the SSG model. Substituting such a linear model in Eq. (4) completes ASM. The explicit solution to Eq. (4), EASM, takes the form :

$$\begin{aligned}b_{ij}^*=C_\eta\{&S_{ij}^*+(S_{ik}^*W_{kj}^*+S_{jk}^*W_{ik}^*)\\&-2\left(S_{ik}^*S_{kj}^*-\frac{1}{3}S_{mn}^*S_{nm}^*\delta_{ij}\right)\}\end{aligned} \tag{6}$$

where

$$\begin{aligned}&b_{ij}^*=\left(\frac{C_3-2}{C_2-\frac{4}{3}}\right)b_{ij}, \qquad C_\eta=\left(-1+\frac{2}{3}\eta_1+2\eta_2\right)^{-1}\\&S_{ij}^*=\frac{1}{4}g\tau(2-C_3)S_{ij}, \qquad W_{ij}^*=\frac{1}{4}g\tau(2-C_4)W_{ij}\\&\eta_1=S_{ij}^*S_{ji}^*, \qquad \eta_2=W_{ij}^*W_{ji}^*\\&g=\left(\frac{1}{2}C_1+P/\varepsilon-1\right)^{-1}, \quad \tau=k/\varepsilon\end{aligned} \tag{7}$$

Eq. (6) is valid for two-dimensional mean flows. See Gatski & Speziale (1993) for an extension of EASM to three-dimensional mean flows. For different versions of EASM, see also Taulbee (1992) which includes nonlocal convection effects, and Wallin and Johanson (2000) which gives a fully explicit solutions, respectively.

The simplest way to check whether EASM is the exact solution of ASM is a direct inversion of Eq. (4) without appealing to Smith's representation theory followed by comparison of the results with Eq. (6). Actually, the application of tensor representation theory lies in the center of controversy, as mentioned above. Thus, this procedure will also verify the validity of the representation with the strain rate and the rotation rate tensors as the independent basis tensors. A general algebraic set yields a full, 5×5 matrix by invoking zero trace for b_{ij} for a point, which can be inverted with Mathematica™ (Wolfram,

1988). The results are compared with the EASM given by Eq. (6), revealing that two models are exactly the same at least for two-dimensional mean flows, contrary to the implication of W97.

For example, the analytical solution of Eq. (4) to the channel flow problem, which has only one non-zero mean-velocity component and inhomogeneous direction, is easily obtained by a direct inversion of a 3×3 matrix which takes the form:

$$\begin{pmatrix} 1 & -A_{12} & 0 \\ -B_{11} & 1 & -B_{22} \\ 0 & -C_{12} & 1 \end{pmatrix}\begin{pmatrix} b_{11} \\ b_{12} \\ b_{22} \end{pmatrix}=\begin{pmatrix} 0 \\ B_c \\ 0 \end{pmatrix} \tag{8}$$

where

$$A_{12}=G\left(\frac{2C_3}{3}-2C_4-\frac{16}{3}\right),\ B_{11}=G(C_3-C_4)$$
$$B_{22}=G(C_3+C_4-4),\qquad B_c=G\left(C_2-\frac{4}{3}\right) \tag{9}$$
$$C_{12}=G\left(\frac{2C_3}{3}-2C_4+\frac{8}{3}\right),\ G=\frac{1}{4}g\tau\left(\frac{dU}{dy}\right)$$

The solution to Eq. (8) is

$$b_{11}=\frac{A_{12}B_c}{1-A_{12}B_{11}-B_{22}C_{12}}$$
$$b_{12}=\frac{B_c}{1-A_{12}B_{11}-B_{22}C_{12}} \tag{10}$$
$$b_{22}=\frac{C_{12}B_c}{1-A_{12}B_{11}-B_{22}C_{12}}$$

b_{33} is automatically given by $b_{33}=-b_{11}-b_{22}$. The comparison of b_{12} terms, for example, shows

$$b_{12}^{ASM}=b_{12}^{EASM}$$
$$=\frac{\left(C_2-\frac{4}{3}\right)G}{1-\left\{\frac{(C_3-2)^2}{3}-(C_4-2)^2\right\}(4G^2)} \tag{11}$$

This result allows us to reconsider the proposal due to W97. Theorem 4 and 5 of W97 that provide the main issues regarding EASM are summarized as follows:

Theorem 4. *Velocity gradient tensor affects* $\overline{u_iu_j}$ *only through* S_{ij}.

Theorem 5. *Each of three eigenvectors of* S_{ij} *is also an eigenvector of* $\overline{u_iu_j}$.

These are strictly derived from PMFI. However, the fact that EASM is the exact, hence the unique, solution of ASM implies that there exists no way of eliminating the terms involved in the rotation-rate tensor in the expression of $\overline{u_iu_j}$, as far as the Reynolds stress equation is a predecessor of EASM, by which EASM differs from NLEVM. It means that both ASM and EASM violate PMFI by Theorem 4, and thus Theorem 5 of W97. But, it is not surprising because both the Navier-Stokes equations and the Reynolds stress transport equations come from Newton's second law of motion, which are not valid for a non-inertial frame of reference.

Recently, Spalart and Speziale (1999) also addressed the issues generated by W97. They contradicted Theorem 4 of W97 in that the Reynolds stress model cannot account for the effect of solid body rotation without the inclusion of W_{ij}. They additionally showed through the observation of the experiment and DNS data that the eigenvectors of $\overline{u_iu_j}$ and S_{ij} do not coincide with each other even in simple channel flow, which is a counter-example of Theorem 5. In this study, we added another counter-example against W97 and thus against PMFI *via* the inspection of ASM and EASM. Consequently, it can be concluded, at odds with W97 and other papers before it (Speziale, 1979), that PMFI rapidly leads to conflicts with accepted facts, is not a property of turbulence, and is not a proper constraint to impose on turbulence models. Actually, it seems to be one of the redundant constraints originated from continuum mechanics, which the Reynolds stress does not really satisfy.

On the other hand, real constraints for the Reynolds stress are coordinate invariance and Galilean invariance, or the principle of observer transformation. Because velocity fluctuation obeys them, the Reynolds stress tensor also does. Recently, Girimaji (1997) reported that EASM due to Gatski & Speziale (1993) violates Galilean invariance, and it is the cause for poor prediction of the rotating channel flow. This specific issue needs further investigation and will be the topic of our future research.

4. An a Priori Test of EASM and Scale Equations

In this section, the original EASM is critically

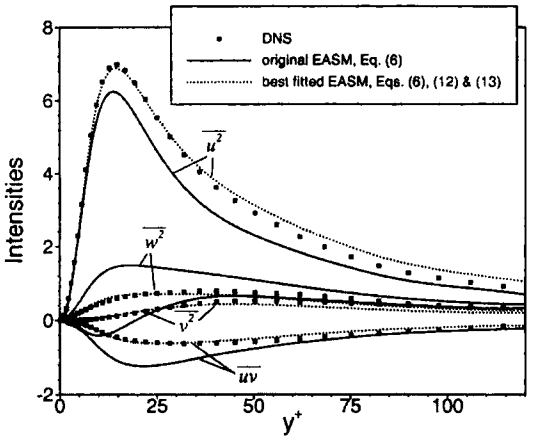

(a) Reynolds stress components

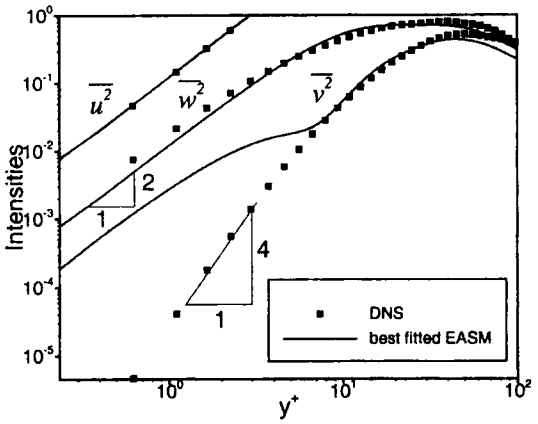

(b) Near-wall behavior of best-fitted results by Eqs. (12) and (13)

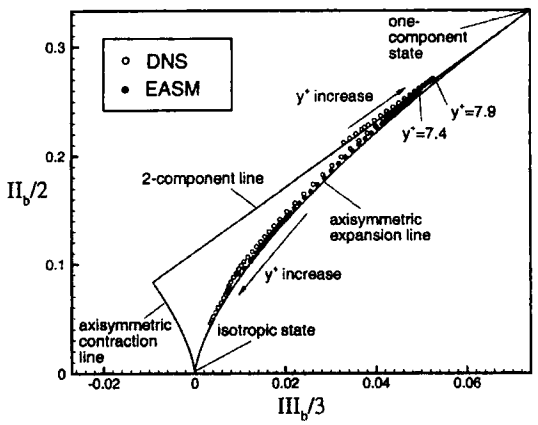

(c) Anisotropy invariant map for b_{ij} at various y^+ in the channel

Fig. 2 An a priori test of EASM in comparison with the DNS database

evaluated on the channel flow followed by the evaluation of the model performance of scale equations *via* the methodology due to Parneix et al. (1998).

Figure 2(a) shows a typical result of an a priori test of model prediction of ASM/EASM without modification as well as empirically fitted results which will be discussed later in this section. This test is necessary to get information on the direction of improvement. Mean velocity, production, turbulent kinetic energy, and dissipation rate are given by the DNS data for this test. The model gives acceptable results far from the wall, whereas it does not reproduce a correct near-wall behavior at all, especially for $\overline{v^2}$, predicting negative values in the viscous sublayer. Two major reasons may be given for this discrepancy, which are equilibrium hypothesis itself and over-prediction of the pressure-strain term in the log layer, since the EASM is derived on the basis of homogeneous flows excluding any inhomogeneity such as the presence of the wall. For the first attempt to improve model prediction based on ad hoc empiricism, the coefficients for the pressure-strain model is tuned. This procedure can be justified by invoking the fact that these are originally calibrated regarding homogeneous shear flows. Time scale τ defined in Eq. (7) has been also modified to meet physical constraints by introducing the Kolmogorov scale (Durbin, 1991 and 1993) in a blending form:

$$T=\sqrt{\left(\frac{k}{\varepsilon}\right)^2+C_T^2\frac{\nu}{\varepsilon}} \tag{12}$$

where C_T is set to be 6.0. Coefficients for the SSG model has been modified such that

$$\begin{aligned} &C_1=3.4(1+P/\varepsilon), \quad C_2=0.8(1-II_b^{1/2}) \\ &C_3=0.65, \qquad\qquad C_4=0.40 \end{aligned} \tag{13}$$

This modification gives best-fitted results in comparison with the DNS data. However, this procedure cannot be generalized for complex flows. More serious problem lies in predicting the near-wall limiting behavior, which is shown in Fig. 2 (b). All the predicted data show isotropic $O(y^2)$ behavior regardless of components. This anomaly cannot be corrected without imposing exact limi-

ting behavior as the boundary conditions. Figure 2(c) represents anisotropy invariant map for the model and the DNS data. The model prediction has no point on the two component line as the result of poor prediction of the near-wall limiting behavior of the wall-normal velocity component.

Next, the model behavior for the scale equations are also investigated. In the light of the methodology given by Parneix et al. (1998), the turbulent kinetic energy and dissipation rate equations are solved, keeping the production term being the same as the DNS data:

$$\frac{Dk}{Dt}=P^{DNS}-\varepsilon+\frac{\partial}{\partial x_l}\left(\nu+\frac{\nu_T}{\sigma_k}\right)\frac{\partial k}{\partial x_l} \tag{14}$$

$$\frac{D\varepsilon}{Dt}=\frac{C_{\varepsilon 1}P^{DNS}-C_{\varepsilon 2}\varepsilon}{T}+\frac{\partial}{\partial x_l}\left(\nu+\frac{\nu_T}{\sigma_\varepsilon}\right)\frac{\partial \varepsilon}{\partial x_l} \tag{15}$$

where T is the time scale defined by Eq. (12), eddy viscosity ν_T is given by

$$\nu_T=C_\mu\overline{v^2}^{DNS}T \tag{16}$$

and $C_\mu=0.2$. Other closure coefficients are given similar values as in Durbin (1991), which are tuned for the channel flow at a higher Reynolds number ($Re_\tau=395$) and are listed in Table 1. No-slip condition is imposed on the wall for k and the Neumann condition is applied at the center of the channel. The boundary condition for the dissipation rate is based on total production-equal-to-dissipation assumption. The model predictions compared with the DNS data for k and ε are shown in Figs. 3(a) and 3(b), where the results at $Re_\tau=395$ are also plotted.

The agreement between the model prediction and the DNS data is quite good for both Reynolds numbers, although the profile of ε has a wiggle near the wall which is larger than the data exhibit. That is, from Fig. 3(b), we can see that the predicted values of ε decay faster than those from DNS near the wall at both Reynolds numbers. This may be due to somewhat small correlation length dominated by the Kolmogorov time scale near the wall. Therefore, the wiggle comes from such a fast decay of ε in the viscous sublayer in conjunction with the enforced boundary condition for ε by which its integrated value in the domain, or the total dissipation, is fixed as

Table 1 Coefficients in k-ε equation and pressure-strain model

k-ε equation	$\sigma_k=1.3$, $\sigma_\varepsilon=1.6$, $C_\mu=0.2$, $C_{\varepsilon 1}=1.62$, $C_{\varepsilon 2}=1.9$	
SSG model	$C_1=3.4+1.8P/\varepsilon$, $C_3=1.25$,	$C_2=0.8-1.3\Pi_b^{1/2}$ $C_4=0.4$

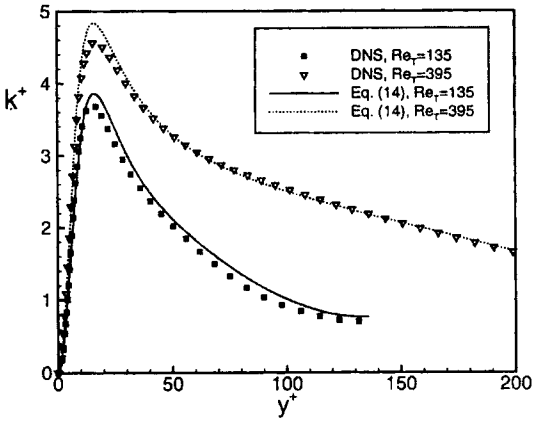

(a) Turbulent kinetic energy

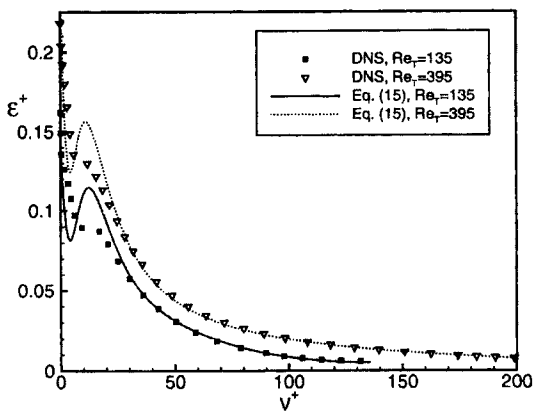

(b) Dissipation rate

Fig. 3 Model predictions for a differential a priori test of scaling variables

that from DNS data. The results from Durbin (1991)'s channel flow computation at $Re_\tau=180$ and $Re_\tau=395$ also show similar wiggles in the profile of ε near the wall. Although numerical test indicates that a larger value of C_T in Eq. (12) can cure this erroneous behavior, no further modification is tried because Eq. (15) is proven to exhibit sufficient generality even for more complex flows, such as the flow over a backward-

facing step (Parneix et al., 1998).

5. Closure for Redistribution and Dissipation Rate Anisotropy

Recently, Manceau et al. (2001) investigated the validity of the hypothesis used to model the pressure term with elliptic relaxation by using a DNS database for the channel flow at $Re_\tau=590$. They showed that the correlation function involving the fluctuating velocity and the Laplacian of the pressure gradient, which is modeled by an exponential function, is actually not isotropic. They also showed that it is not only elongated in the streamwise direction but also asymmetric in the wall-normal direction. This feature is considered to be the main cause for slight amplification of the redistribution between the Reynolds stress components in the log layer as predicted by a symmetric operator. The objective of this section is to confirm the observation of Manceau et al. (2001) for a lower Reynolds number channel flow.

On the other hand, inspecting the budget in the Reynolds stress equation reveals that reproducing the limiting behavior of $\phi_{ij}-\varepsilon_{ij}$ is crucial in predicting the correct behavior of $\overline{u_iu_j}$. In this section, the low-Reynolds number models for the pressure redistribution and dissipation rate are investigated in detail.

The original velocity-pressure term, which is given by $\phi_{ij}=-\frac{1}{\rho}(\overline{u_jp_{,i}}+\overline{u_ip_{,j}})$, is represented by using an approximate Green function H.

$$\rho\phi_{ij}(\boldsymbol{x})=-\int_\Omega(\overline{u_j(\boldsymbol{x})\nabla^2p_{,i}}+\overline{u_i(\boldsymbol{x})\nabla^2p_{,j}})H(\boldsymbol{x},\boldsymbol{x}')dV(\boldsymbol{x}') \quad (17)$$

$$H(\boldsymbol{x},\boldsymbol{x}')=\frac{1}{4\pi\|\boldsymbol{x}'_0-\boldsymbol{x}\|}+\frac{1}{4\pi\|\boldsymbol{x}'_{-1}-\boldsymbol{x}\|}+\frac{1}{4\pi\|\boldsymbol{x}'_1-\boldsymbol{x}\|} \quad (18)$$

where the three terms on the right-hand side (RHS) of Eq. (18) are the principal, first image and second image terms, and $\boldsymbol{x}'_{-1}$ and $\boldsymbol{x}'_1$ are the images of $\boldsymbol{x}'_0$ in the walls located at $y=0$ and $y=1$, respectively. The image terms are often referred to as "wall echo" or "wall reflection". Since Launder et al. (1975) it has been widely accepted that wall echo is responsible for the reduction in the amplitude of the energy redistribution between components of the Reynolds stress.

In Eq. (17), two-point correlations between the fluctuating velocity and the Laplacians of the pressure gradient appear, and they can be modeled as (Durbin, 1991)

$$\overline{u_n(\boldsymbol{x})\nabla^2p_{,m}(\boldsymbol{x}')}=\overline{u_n(\boldsymbol{x}')\nabla^2p_{,m}(\boldsymbol{x}')}\exp\left(-\frac{\|\boldsymbol{x}'-\boldsymbol{x}\|}{L}\right) \quad (19)$$

where L is the correlation length scale. The velocity-pressure is the solution of the following Yukawa equation.

$$\phi_{ij}-L^2\nabla^2\phi_{ij}=-\frac{L^2}{\rho}(\overline{u_j\nabla^2p_{,i}}+\overline{u_i\nabla^2p_{,j}}) \quad (20)$$

Durbin proposed to use a quasi-homogeneous model such as the LRR model or the SSG model instead of the RHS of Eq. (20). This leads to the following elliptic relaxation model for ϕ_{ij}:

$$\phi_{ij}-L^2\nabla^2\phi_{ij}=\phi^h_{ij} \quad (21)$$

Figures 4(a) and 4(b) show terms in the approximate Green function H given by Eq. (18) for the streamwise and the wall-normal components of the pressure redistribution terms. In this figure, we can see clearly that the image terms are of the same sign as the principal terms. This implies that the image terms actually amplify the redistribution, contrary to the common belief on the effect of wall echo. This result confirms the argument of Manceau et al. (2001) on the channel flow at a relatively high Reynolds number.

Figures. 5(a) and 5(b) show two-point correlation functions for the fluctuating velocity and the Laplacian of the pressure gradient in the streamwise and wall-normal directions, respectively. For this case, separation distance of the correlation for the streamwise and spanwise directions is zero. Vertical dotted lines indicate the lines of zero separation, i.e., the lines of symmetry. It is shown that the anisotropy between the streamwise and wall-normal directions is the main characteristic of the correlation functions as well as asymmetry. The degree of anisotropy is more amplified than the results of Manceau et al. (2001) including large negative correlation re-

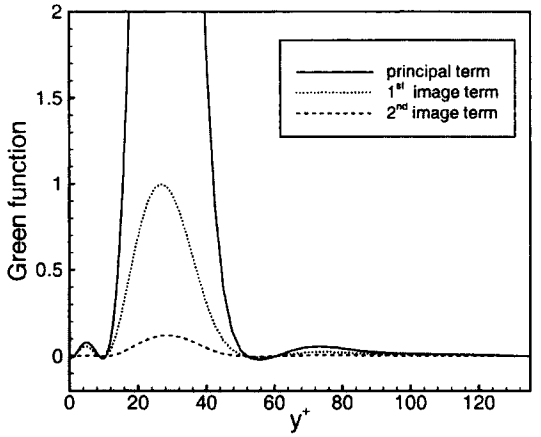

(a) $\overline{u_1(\boldsymbol{x})\nabla^2 p_{,1}(\boldsymbol{x}')}/\| \boldsymbol{x}'_n - \boldsymbol{x} \|$

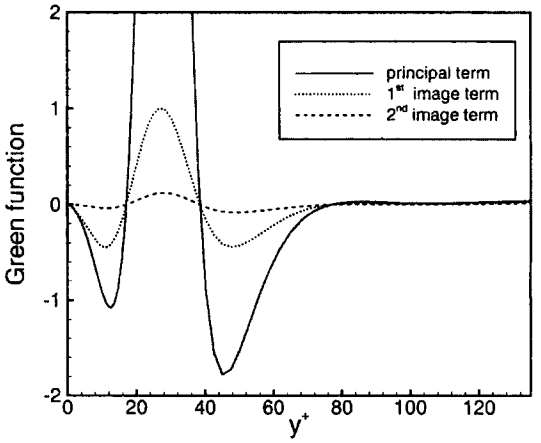

(b) $\overline{u_2(\boldsymbol{x})\nabla^2 p_{,2}(\boldsymbol{x}')}/\| \boldsymbol{x}'_n - \boldsymbol{x} \|$

Fig. 4 Terms in approximate Green functions for redistribution terms

gion for the wall-normal component. This may be the reason why the predictability of the $k-\varepsilon-v^2$ model gets worse as the Reynolds number decreases.

By considering the asymmetry of the correlation function in the wall-normal direction, Manceau and Hanjalic (2000) proposed an asymmetric operator (denoted as MH operator, hereinafter):

$$\phi_{ij} - L^2\nabla^2\phi_{ij} - 8L^3\nabla L\cdot\nabla\frac{\phi_{ij}}{L^2} = \phi^h_{ij} \qquad (22)$$

Figure 5(c) compares elliptic models, symmetric Yukawa and unsymmetric MH operators for the correlation function at $y^+=7$ and $y^+=50$. This also shows that the unsymmetric model reproduces a correct asymmetry in the correlation

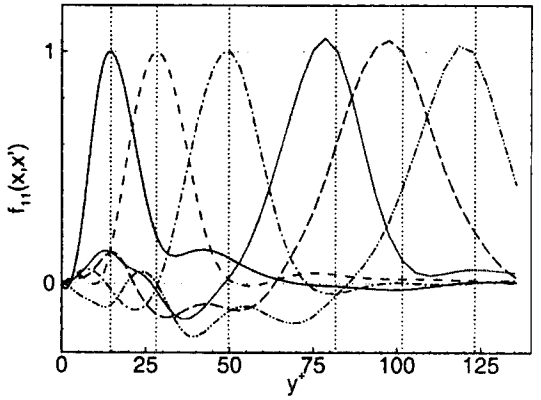

(a) $\overline{u_1(\boldsymbol{x})\nabla^2 p_{,1}(\boldsymbol{x}')}/\overline{u_1(\boldsymbol{x}')\nabla^2 p_{,1}(\boldsymbol{x}')}$

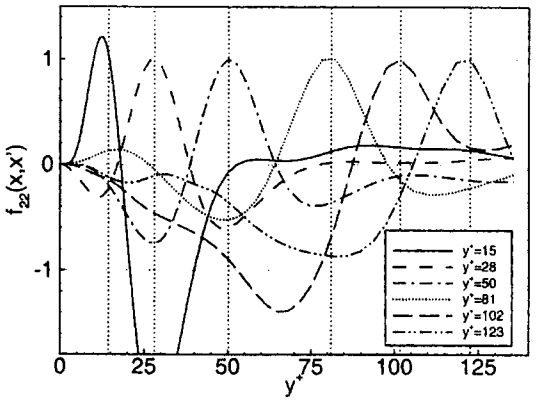

(b) $\overline{u_2(\boldsymbol{x})\nabla^2 p_{,2}(\boldsymbol{x}')}/\overline{u_2(\boldsymbol{x}')\nabla^2 p_{,2}(\boldsymbol{x}')}$

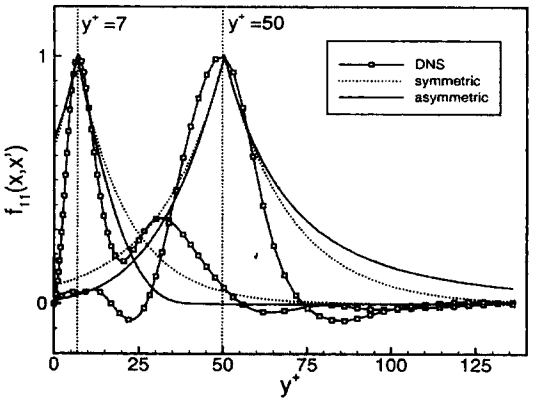

(c) $\overline{u_1(\boldsymbol{x})\nabla^2 p_{,1}(\boldsymbol{x}')}/\overline{u_1(\boldsymbol{x}')\nabla^2 p_{,1}(\boldsymbol{x}')}$; elliptic models for the correlation function

Fig. 5 Two-point correlation functions in the pressure-strain term (vertical dotted lines indicate zero separation distance)

function. However, we can also see that the shape of the correlation function modeled by both

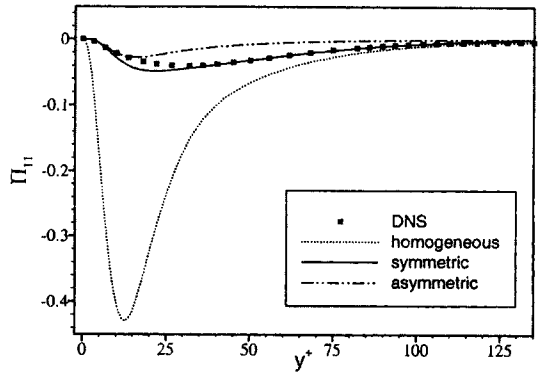

(a) $II_{11}=\phi_{11}-\varepsilon_{11}+\frac{\overline{u_1u_1}}{k}\varepsilon$

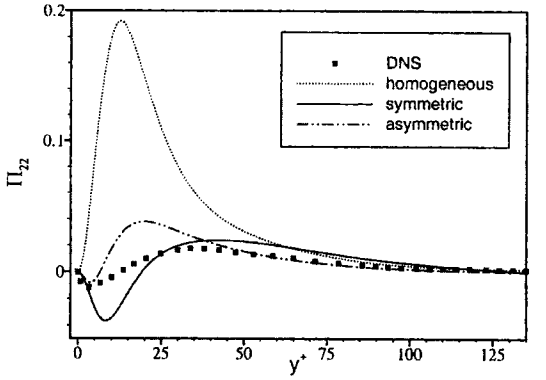

(b) $II_{22}=\phi_{22}-\varepsilon_{22}+\frac{\overline{u_2u_2}}{k}\varepsilon$

Fig. 6 Effect of elliptic relaxation on the prediction of the pressure-redistribution terms

elliptic models are somewhat too simple to reproduce all the features of the correlation function correctly.

Figures 6(a) and 6(b) represent the model prediction and the DNS data for some components of $\phi_{ij}-\varepsilon_{ij}+\frac{\overline{u_iu_j}}{k}\varepsilon$ term, which was used by Durbin (1993) to construct the Reynolds stress model instead of usual decomposition shown in Eq. (3). MH operator generally decays faster than Yukawa operator for 11-component. Thus, Yukawa operator is in closer agreement with the DNS data. However, this does not mean the failure of the asymmetric operator because all the coefficients for time and length scales are originally fitted to symmetric operators. Moreover, the homogeneous model is not the exact one-point correlation of the velocity fluctuation and the Laplacian of the pressure gradient. MH operator outperforms Yukawa operator when the asymptotic boundary condition is given at the wall (Durbin, 1993) as shown in Fig. 6(b).

Next, the model for the dissipation rate anisotropy is considered because the dissipation rate, in general, has a strong degree of anisotropy, which will be included in the construction of a new composite algebraic stress model. The available models are due to Speziale & Gatski (1997, SG model) and Hallback et al. (1990, HGJ model). Although other models, such as the model due to Hanjalic and Jakirlic (1993), can be easily incorporated, they are not considered here due to the dependency of such models on empirical functions of the turbulence Reynolds number. In fact, only HGJ model is adopted in this study because the a priori test results for both models using the DNS data reveal that SG model predicts surprisingly inaccurate values for the dissipation rate anisotropy, whereas the results from HGJ model is within an acceptable range. HGJ model is given by

$$d_{ij}=\left[1+\alpha\left(2b_{nm}b_{mn}-\frac{2}{3}\right)\right]b_{ij} -2\alpha\left(b_{ik}b_{kj}-\frac{1}{3}b_{nm}b_{mn}\delta_{ij}\right) \tag{23}$$

where $d_{ij}=\varepsilon_{ij}/(2\varepsilon)-\frac{1}{3}\delta_{ij}$ is the dissipation rate anisotropy tensor, and α is a free parameter which has a lower bound of zero and an upper bound of unity to meet physical constraints between the stress and dissipation rate anisotropy. The original value of α is 3/4, which comes from the RDT analysis of homogeneous shear flow. However, the value 1/4 gives a closer agreement with the DNS data than the original value (Figs. 7(a) and 7(b)) for the normal components. The simple approximation $\varepsilon_{ij}=\frac{\overline{u_iu_j}}{k}\varepsilon$, i.e., $d_{ij}=b_{ij}$, which is used by Durbin (1993), is regarded as a special case when $\alpha=0$. It is obvious from Fig. 7 that the DNS results lie between those obtained by $\alpha=0$ and $\alpha=3/4$, and an optimal value for α exists within this range for the channel flow under consideration.

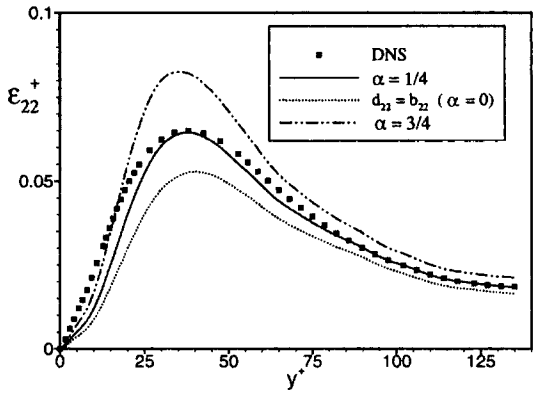

(a) ε_{22}

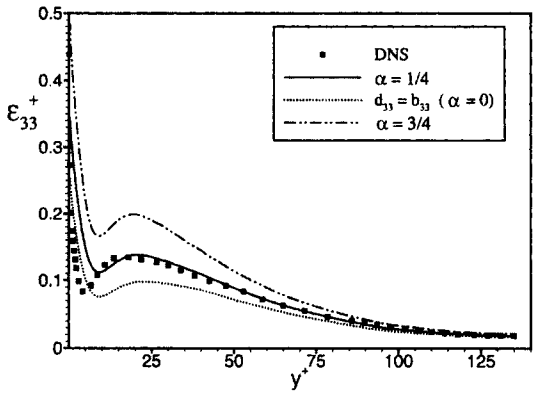

(b) ε_{33}

Fig. 7 Prediction of the dissipation rate components with HGJ model

6. A Novel Composite Stress Model

In this section, a novel composite algebraic stress model is proposed. The key idea is to isolate the pressure-redistribution term as an independent tensor. This assumption can be justified by the fact that the pressure-redistribution term is in itself a two-point correlation, and thus it cannot be represented by single point values, being independent of the local strain (S_{ij}) and rotation rate (W_{ij}). A similar approach was adopted by Adumitroaie et al. (1999) for a compressible version of EASM by introducing the baroclinic dyad tensor composed of the pressure and density gradients as the independent tensor. The realization of this idea, however, is not straightforward due to the following difficulties:

1. The singularity of a leading coefficient analogous to g in Eqs. (7) and (9) may occur when P/ε approaches unity. This comes from the implicit treatment of the redistribution term, whereas Rotta's return-to-isotropy constant C_1 contained in g prevents it in the original EASM.
2. The introduction of dissipation rate anisotropy model leads to a nonlinear ASM.
3. According to the representation theory, the presence of three independent tensors, S_{ij}, W_{ij} and Φ_{ij}, results in 41 integrity basis tensors, which is out of practical range. Therefore, no direct inversion nor tensor representation can be used to get an EASM.

Among them, the singularity problem can be easily cured by replacing the equilibrium hypothesis with that proposed by Taulbee (1992). Then, Eq. (3) can be written as

$$2k\frac{Db_{ij}}{Dt}=-\frac{\overline{u_iu_j}}{k}(P-\varepsilon)+P_{ij}+\Phi_{ij}-\varepsilon_{ij} \quad (24)$$

The ASM Eq. (3) is recovered invoking $Db_{ij}/Dt=0$ at the equilibrium state. To account for nonlocal convective effect, Taulbee (1992) expanded Db_{ij}/Dt in the Taylor series with time scale (T) and strain rate ($\sigma=\sqrt{S_{nm}S_{mn}}$). For small $T\sigma$, the equilibrium condition $Db_{ij}/Dt=0$ is approximated by

$$\frac{D}{Dt}\left(\frac{b_{ij}}{T\sigma}\right)=0 \quad (25)$$

Substitution of Eq. (25) into Eq. (24) and rewriting it in basic tensors leads to

$$\begin{aligned}T\sigma\frac{D}{Dt}\left(\frac{b_{ij}}{T\sigma}\right)=&-\left(\frac{P}{\varepsilon}-1+\frac{1}{\sigma}\frac{DT\sigma}{Dt}\right)\frac{b_{ij}}{T}-\frac{2}{3}S_{ij}\\&-\left(b_{ik}S_{jk}+b_{jk}S_{ik}-\frac{2}{3}b_{mn}S_{mn}\delta_{ij}\right)\\&-(b_{ik}W_{jk}+b_{jk}W_{ik})+\frac{1}{2k}\Phi_{ij}-\frac{1}{T}d_{ij}\end{aligned} \quad (26)$$

where the convection term $\frac{1}{\sigma}\frac{DT\sigma}{Dt}$ is approximated by

$$\frac{1}{\sigma}\frac{DT\sigma}{Dt}=\frac{T}{\sigma}\frac{D\sigma}{Dt}+(C_{\varepsilon_2}-1)-(C_{\varepsilon_1}-1)\frac{P}{\varepsilon} \quad (27)$$

Eq. (27) is derived from the $k-\varepsilon$ equation, Eqs. (14) and (15), neglecting diffusion terms and

setting $T=k/\varepsilon$. Taulbee (1992) showed that the term $\frac{T}{\sigma}\frac{D\sigma}{Dt}$ drastically improves the predictability of (E)ASM for time varying, homogeneous shear flows. But, for a fully developed channel flow it is automatically zero. However, the remaining terms still play an important role in preventing the singularity of the leading coefficient that is multiplied by b_{ij}/T in Eq. (26), otherwise the coefficient would be simply $P/\varepsilon-1$, which must be zero somewhere in the domain. An algebraic stress model is achieved by setting the LHS of the Eq. (26) zero. Combining closure models for the dissipation rate anisotropy and substituting Eq. (27) into Eq. (26), a new composite stress model is constructed, resulting in a set of nonlinear equations:

$$\begin{aligned} b_{ij}=&-\beta_1 S_{ij}+\beta_2\left(b_{ik}b_{kj}-\frac{1}{3}b_{mn}b_{nm}\delta_{ij}\right)\\ &-\beta_3\left(b_{ik}S_{jk}+b_{jk}S_{ik}-\frac{2}{3}S_{mn}b_{mn}\delta_{ij}\right)\\ &-\beta_4\left(b_{ik}W_{jk}+b_{jk}W_{ik}\right)+\beta_5\Pi_{ij} \end{aligned} \tag{28}$$

where $\beta_1=\frac{2}{3}gT$, $\beta_2=2g\alpha$, $\beta_3=\beta_4=gT$, $\beta_5=T/2g$, with $\alpha=1/4$, $\Pi_{ij}=\Phi_{ij}/k$, and T is as given by Eq. (12). Now, the coefficient g is given by

$$g=\left(P/\varepsilon+2a\Pi_b-\frac{2}{3}a+\omega\right)^{-1} \tag{29}$$

where $\omega=(1-C_{\varepsilon 1})P/\varepsilon+(C_{\varepsilon 2}-1)+(T/\sigma)(D\sigma/Dt)$ is a newly introduced term. It can be easily shown that g is always positive for all possible values of P/ε and Π_b due to the inclusion of ω. Π_{ij} is then determined by an elliptic relaxation procedure with the asymmetric MH operator as discussed in the previous section:

$$\Pi_{pq}-L_{pq}^2\nabla^2\Pi_{pq}-8L_{pq}^3\nabla L_{pq}\cdot\nabla\frac{\Pi_{pq}}{L_{pq}^2}=\Pi_{pq}^h \tag{30}$$

Note that the summation convention is not applied here. The original asymmetric model is modified to account for the anisotropy in the correlation function through the length scale L_{pq} in each principal direction, which is given by

$$L_{pq}=C_{Lpq}\sqrt{(k^{3/2}\varepsilon^{-1})^2+C_{\eta pq}^2(\nu^{3/4}\varepsilon^{-1/4})^2} \tag{31}$$

Coefficients C_{Lpq} and $C_{\eta pq}$ are calibrated by differential a priori tests of Eq. (30) with the present DNS database at $Re_\tau=135$. The SSG model is used as single-point correlation, i.e., the RHS of Eq. (30) using original constants as listed in Table 1. C_{Lpq} and $C_{\eta pq}$ are listed in Table 2. Also listed are isotropic coefficients, C_L and C_η for Durbin's $k-\varepsilon-v^2$ model (Durbin, 1991). It is seen from Table 2 that the constants are a bit larger than those for the $k-\varepsilon-v^2$ model because coefficients are calibrated on asymmetric operator.

Table 2 Coefficients in a new composite EASM

EASM/ER	$C_{L11}=C_{L33}=0.4$, $C_{L12}=0.3$, $C_{L22}=0.2$ $C_{\eta 11}=C_{\eta 33}=120$, $C_{\eta 12}=130$, $C_{\eta 22}=150$
$k-\varepsilon-v^2$ model	$C_L=0.2$, $C_n=80$

Required boundary conditions (Manceau & Hanjalic, 2002) can be imposed on the wall through the redistribution terms and dissipation rate.

$$\begin{aligned} \Pi_{ij}^w&=-\frac{20\nu^2}{\varepsilon}\frac{\overline{u_iu_j}}{y^4}, && ij=22,\ 12,\ 23\\ \Pi_{ij}^w&=-\frac{1}{2}\Pi_{22}^w, && ij=11,\ 33\\ \Pi_{ij}^w&=0,\quad \varepsilon=2\nu\frac{k}{y^2} \end{aligned} \tag{32}$$

Obviously, Eq. (32) needs to be written in a general, frame-independent form by identifying the direction normal to the wall, to be applicable to complex geometry and multiple walls, so that this extension is underway. The method proposed by Manceau & Hanjalic (2002) may be a possible choice. In any event, these boundary conditions insure proper near-wall limiting behavior of $\phi_{ij}-\varepsilon_{ij}$. For example, in the near-wall budget of $\overline{v^2}$, $\phi_{22}-\varepsilon_{22}$ becomes

$$\phi_{22}-\varepsilon_{22}\approx k\Pi_{22}-\frac{\overline{v^2}}{k}\varepsilon=-12\nu\frac{\overline{v^2}}{y^2} \tag{33}$$

However, unlike RSM, Eq. (33) does not automatically insure the correct prediction of the limiting behavior of $\overline{v^2}\propto y^4$ because the Reynolds stress components modeled by EASM are not the solutions of differential equations but the solution of a system of algebraic equations, where terms in

the budget of the Reynolds stress are neglected, decomposed and rearranged, so that it is nearly impossible to track the near-wall behavior of each component. Therefore, it should be shown only through the application to numerical simulations.

Now, the solution procedure of the nonlinear system given by Eq. (28) is outlined. Two approaches are proposed to overcome remaining two difficulties. The first is an iterative approach which was originally introduced by Apsley & Leschziner (1998).

Consider the general implicit system

$$\boldsymbol{b}=\boldsymbol{S}+\boldsymbol{f}(\boldsymbol{b}) \tag{34}$$

This may be approximated iteratively by the sequence

$$\boldsymbol{b}^{(1)}=\boldsymbol{S},\ \boldsymbol{b}^{(n)}=\boldsymbol{S}+\boldsymbol{f}(\boldsymbol{b}^{(n-1)}),\ n=1,\ 2,\ 3,\ \cdots \tag{35}$$

If the same technique is applied to the system (28), we obtain:

$$\boldsymbol{b}^{(0)}=-\beta_1\boldsymbol{S} \tag{36}$$

This is obviously a linear eddy viscosity model. For $n=1$, we obtain from Eq. (35),

$$\begin{aligned}\boldsymbol{b}^{(1)}=&-\beta_1\boldsymbol{S}+(\beta_2\beta_1^2+2\beta_1\beta_3)\left(\boldsymbol{S}^2-\frac{1}{3}II_S\boldsymbol{I}\right)\\&+\beta_1\beta_4(\boldsymbol{WS}-\boldsymbol{SW})+\beta_5\boldsymbol{II}\end{aligned} \tag{37}$$

This is a quadratic NLEVM which has tensorially the same form as EASM but the inclusion of Π_{ij} term. $n=2$ in Eq. (35) leads to

$$\begin{aligned}\boldsymbol{b}^{(2)}=&\gamma_1\boldsymbol{S}+\gamma_2\left(\boldsymbol{S}^2-\frac{1}{3}II_S\boldsymbol{I}\right)+\gamma_3(\boldsymbol{WS}-\boldsymbol{SW})\\&+\gamma_4\left(\boldsymbol{W}^2\boldsymbol{S}+\boldsymbol{SW}^2-\frac{2}{3}\{\boldsymbol{WSW}\}\boldsymbol{I}\right)\\&+\gamma_5(\boldsymbol{WS}^2-\boldsymbol{S}^2\boldsymbol{W})\\&+\gamma_6\boldsymbol{II}+\gamma_7\left(\boldsymbol{II}^2-\frac{1}{3}II_{II}\boldsymbol{I}\right)\\&+\gamma_8(\boldsymbol{WII}-\boldsymbol{IIW})\\&+\gamma_9\left(\boldsymbol{IIS}+\boldsymbol{SII}-\frac{2}{3}\{\boldsymbol{IIS}\}\boldsymbol{I}\right)\end{aligned} \tag{38}$$

where

$$\begin{aligned}\gamma_1=&-\beta_1-\frac{1}{3}(\beta_2\beta_1^2+2\beta_1\beta_3)\beta_4II_S\\&-2(\beta_1+3\beta_1\beta_4)II_W\\\gamma_2=&2\beta_1\beta_3,\ \gamma_3=\beta_1\beta_4,\ \gamma_4=-3\beta_1\beta_4\\\gamma_5=&-(\beta_2\beta_1^2\beta_3+2\beta_1\beta_3^2+\beta_1\beta_4^2)\\\gamma_6=&\beta_5,\ \gamma_7=\beta_2\beta_5^2,\ \gamma_8=-\beta_4\beta_5,\ \gamma_9=-\beta_3\beta_5\end{aligned} \tag{39}$$

Here, Cayley-Hamilton theorem is applied to S_{ij} and $S_{ij}+W_{ij}$ and bi-quadratic terms are neglected for simplicity. This is a cubic stress-strain relation, and iteration is concluded at this level. Although it seems that too many empirical constants are introduced in the model given by Eq. (38), most of them are from the parent RSM, pressure-strain model, scale equations, etc. They are well-established and verified constants among turbulence modeling community. Only coefficients C_{Lpq} and $C_{\eta pq}$ in Eq. (31) are newly introduced constants in this study, but they are mere anisotropic variants of C_L and C_η in Durbin's $k-\varepsilon-v^2$ model and the Reynolds stress model (Durbin, 1991; Durbin, 1993), which share the same physical and mathematical meaning.

Second approach is to solve the system of nonlinear equations (28) numerically. The numerical solution of this system of nonlinear equation is easily achieved by using the IMSL subroutine NEQMF. The comparison between the above two schemes suggests that the numerical solution method is superior to the iteration method in that the numerical solution approach is always stable and gives accurate result. However, if we are to retain a tensorially explicit form, the iteration method would be preferred. In that sense, the numerical solution method is not an "explicit" algebraic stress model since the explicit solutions of b_{ij} are not sought. However, if we are only interested in the prediction results of the models, the distinction between ASM and EASM is meaningless because these two are the same model as shown in Section 3, and therefore it is only the matter of numerical efficiency. However, we still prefer to call the model as EASM rather than ASM even in view of numerical solution method because it is proposed as the next step to the existing EASMs (Gatski & Speziale, 1993; Taulbee, 1992) that belong to 'new-generation

turbulence model', so that it has a different context from the classical ASM by Rodi (1976).

We will refer to the model developed in this section as EASM/ER (Explicit Algebraic Stress Model with Elliptic Relaxation) to emphasize the elliptic relaxation procedure to obtain the pressure-redistribution terms. The model predictions of EASM/ER for a fully developed channel flow at $Re_\tau = 135$ are given in Figs. 8(a), 8(b), and 8(c). This is the first full numerical simulation without using any DNS data. The calculation is done with a simple one-dimensional, parabolic code, which adopts implicit time integration and 2nd-order central difference for all spatial derivatives. The mean momentum equation and k-ϵ Eq. (14) and (15), in conjunction with the redistribution tensor Eq. (30), are solved simultaneously with block-TDMA solver with the implicit treatment of the boundary conditions. The results from GS-EASM are also shown in Figs. 8 (a) and 8(b) to highlight the superiority of the present model, EASM/ER, in predicting wall-bounded turbulent flows. In this simulation with GS-EASM model, the same scale Eq. (14) and (15), are used in conjunction with the modified time scale T defined by Eq. (12) to make a fair comparison with the present EASM/ER. It should be noted that no wall function nor damping function is used in the present GS-EASM model simulation, whereas Gatski & Speziale (1993) adopted the wall function for the computation of the rotating channel flow.

The results from EASM/ER are in excellent agreement for both the mean velocity and the Reynolds stress components except for small overprediction of $\overline{uv}$ (in absolute values) and its gradient, which results in small underprediction of the mean velocity in the buffer layer. Whereas, those from GS-EASM highly underpredicts the mean velocity as a result of the overprediction of the gradients of $\overline{uv}$. The prediction of anisotropies in the normal components are not satisfactory with GS-EASM either. Note that the actual model prediction of GS-EASM is completely different from those with the a priori test as shown in Fig. 2(a). This again reminds us that caution is required in interpreting the model

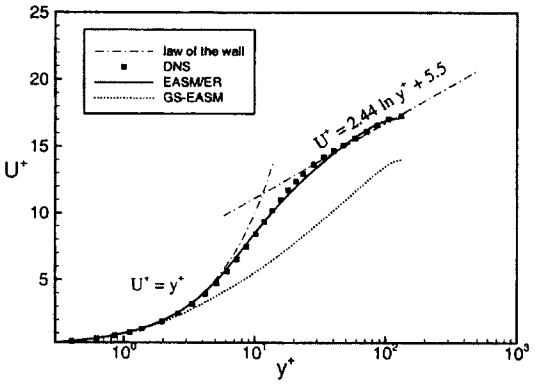

(a) Mean streamwise velocity

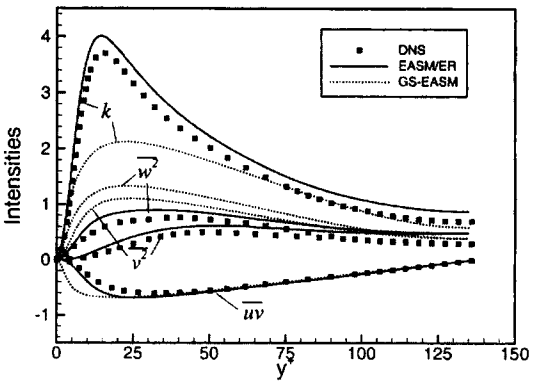

(b) Reynolds stress

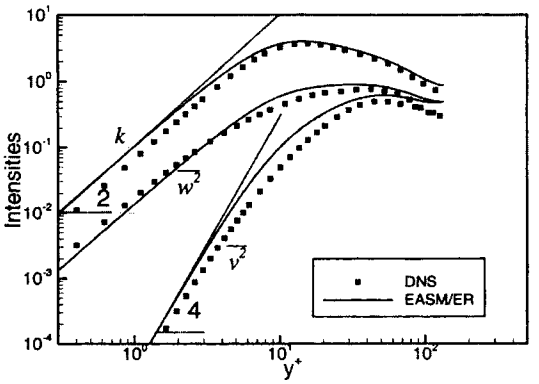

(c) Near-wall limiting behavior

Fig. 8 Predictions by the new composite algebraic stress model

predictions from an a priori test because they are only conditional results provided that other variables, such as the mean velocity, are not influenced by the model prediction. Figure 8(c) shows the limiting behaviors of the Reynolds stress. From the figure, it is clear that the model

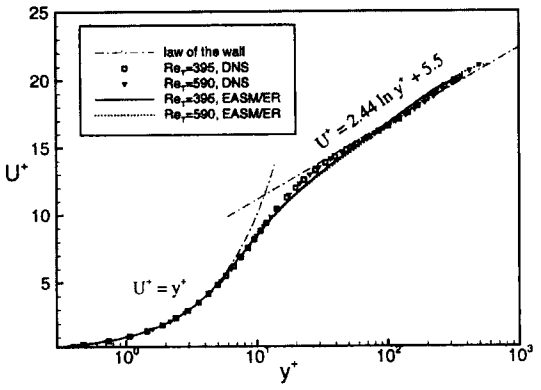

(a) Mean streamwise velocity

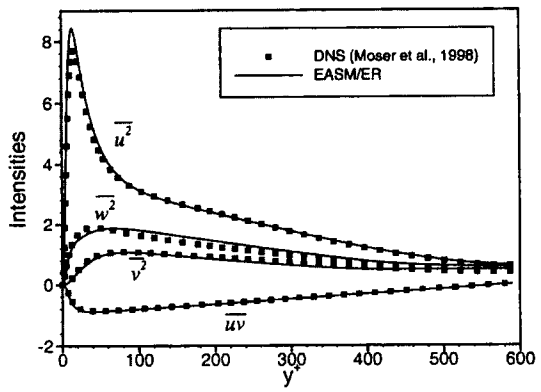

(b) Reynolds stress at $Re_\tau=590$

Fig. 9 Predictions by the new composite algebraic stress model at higher Reynolds numbers

predicts exact $O(y^2)$ limiting behavior for k and $\overline{w^2}$, and $O(y^4)$ behavior for $\overline{v^2}$.

The model is applied to the channel flows at higher Reynolds numbers to check the generality of the model constants, which were tuned at $Re_\tau=135$, as well as the model performance itself. Figure 9(a) shows the mean streamwise velocities predicted by EASM/ER at $Re_\tau=395$ and $Re_\tau=590$ in comparison with the results from the DNS database of Moser et al. (1998). Good agreements in mean velocities are also achieved at these higher Reynolds numbers. The model predictions of the Reynolds stress components at $Re_\tau=590$ are shown in Fig. 9(b). We can see again an excellent agreement with the DNS data. It is interesting to note that the model predictions get closer to the DNS results as the Reynolds number increases although the model is mainly calibrated for the low-Reynolds number flow. This implies the inherent capability of (E) ASM for capturing the stress anisotropy at the equilibrium state far from the wall.

However, the solution procedure becomes much more complex than simple EASM because solving the nonlinear equations and the elliptic equations for each component of II_{ij} is obviously a non-trivial job for complex flows. Therefore, the main virtue of EASM may be lost during this modification. Moreover, the model contains a bit too many adjustable constants. However, the model has only finite degrees of freedom and the differential and algebraic model equations determine the profile of the turbulence statistics. This contrasts to the infinite degrees of freedom in the damping function, which are used to fit the entire mean velocity profile.

6. Conclusions

Through the present investigation, the following conclusions can be drawn.

First, EASM is proven to be the exact tensor representation of ASM for a two-dimensional flow. Therefore, PMFI can be regarded as a too restrictive constraint on the Reynolds stress.

Second, the result of Manceau et al. (2001) that the pressure-velocity correlation function is anisotropic and asymmetric in the wall-normal direction, is confirmed for low-Reynolds-number flow. It is also confirmed that elliptic relaxation method plays a key role in reducing overprediction of the pressure term in the log layer. Further refinement of pressure-redistribution term must be done in two directions: quasi-homogeneous model to accurately predict the one-point correlation and the correlation function between the fluctuating velocity and the Laplacian of the pressure gradient in order to reproduce their anisotropy and asymmetry in a systematic way.

Finally, a new nonlinear, composite algebraic stress model is proposed and tested for the channel flow calculation. The model shows the ability to predict correct near-wall behavior and the possibility of incorporating non-local effect within the algebraic framework. However, the

proposed model should be applied to more complex flows, such as the flow over a backward-facing step for the validation of the generality of the model performance. It is the topic of our subsequent research.

Acknowledgment

This work was supported by the Brain Korea 21 Project in 2002.

References

Adumitroaie, V., Ristorcelli, J. R. and Taulbee, D. B., 1999, "Progress in Favre-Reynolds Stress Closures for Compressible Flows," *Phys. Fluids*, Vol. 11, No. 9, pp. 2696~2719.

Apsley, D. D. and Leschziner, M. A., 1998, "A New Low-Reynolds-Number Nonlinear Two-Equation Turbulence Model for Complex Flows," *Int. J. Heat and Fluid Flow*, Vol. 19, pp. 209~222.

Choi, H., Moin, P. and Kim, J., 1993, "Direct Numerical Simulation of Turbulent Flow over Riblets," *J. Fluid Mech.*, Vol. 255, pp. 503~539.

Choi, H. and Moin, P., 1994, "Effects of the Computational Time Step on Numerical Solutions of Turbulent Flow," *J. Comput. Phys.*, Vol. 113, pp. 1~4.

Choi, H., Moin, P. and Kim, J., 1994, "Active Turbulence Control for Drag Reduction in Wall-Bounded Flows," *J. Fluid Mech.*, Vol. 262, pp. 75~110.

Durbin, P. A., 1991, "Near-Wall Turbulence Closure Modeling without Damping Functions," *Theoret. Comput. Fluid Dynamics*, Vol. 3, pp. 1~13.

Durbin, P. A., 1993, "A Reynolds Stress Model for Near-Wall Turbulence," *J. Fluid Mech.*, Vol. 249, pp. 465~498.

Gatski, T. B. and Speziale, C. G., 1993, "On Explicit Algebraic Stress Models for Complex Turbulent Flows," *J. Fluid Mech.*, Vol. 254, pp. 59~78.

Girimaji, S. S., 1997, "A Galilean Invariant Explicit Algebraic Reynolds Stress Model for Turbulent Curved Flows," *Phys. Fluids*, Vol. 9, No. 4, pp. 1067~1077.

Hallback, M., Groth, J. and Johansson, A. V., 1990, "An Algebraic Model for Nonisotropic Turbulent Dissipation Rate in Reynolds Stress Closures," *Phys. Fluids* A, Vol. 2, No. 10, pp. 1859~1866.

Hanjalic, K., 1994, "Advanced Turbulence Closure Models : A View of Current Status and Future Prospects," *Int. J. Heat and Fluid Flow*, Vol. 15, pp. 178~203.

Hanjalic, K. and Jakirlic, S., 1993, "A Model of Stress Dissipation in Second-Moment Closures," *Appl. Scientific Research*, Vol. 51, pp. 513~518.

Kasagi, N., Horiuti, K., Miyake, T., Miyauchi, T. and Nagano, Y., 1992, Establishment of the Direct Numerical Simulation Databases of Turbulent Transport Phenomena, Grant-in-Aid for Cooperative Research No. 02302043, the Ministry of Education, Science and Culture, Japan.

Kuroda, A., 1990, Direct Numerical Simulation of Couette-Poiseuille Flows, Dr. Eng. Thesis, the University of Tokyo.

Kuroda, A., Kasagi, N. and Hirata, M., 1989, "A Direct Numerical Simulation of the Fully Developed Turbulent Channel Flow," International Symposium on Computational Fluid Dynamics, Nagoya, 1989, pp. 1174~1179 ; also in *Numer. Met. Fluid Dyn.*, 1990, Vol. 2, pp. 1012~1017.

Launder, B. E., Reece, G. and Rodi, W., 1975, "Progress in the Development of a Reynolds-Stress Turbulence Closure," *J. Fluid Mech.*, Vol. 68, pp. 537~566.

Lele, S. K., 1992, "Compact Finite Difference Schemes with Spectral-like Resolution," *J. Comp. Phys.*, Vol. 103, pp. 16~42.

Manceau, R. and Hanjalic, K., 2000, "A New Form of the Elliptic Relaxation Equation to Account for Wall Effects in RANS Modelling," *Phys. Fluids*, Vol. 12, No. 9, pp. 2345~2351.

Manceau, R., Wang, M. and Laurence, D., 2001, "Inhomogeneity and Anisotropy Effects on the Redistribution Term in Reynolds-Averaged Navier-Stokes Modelling," *J. Fluid Mech.*, Vol. 438, pp. 307~338.

Manceau, R. and Hanjalic, K., 2002, "Elliptic Blending Model : A New Near-Wall Reynolds-

Stress Turbulence Closure," *Phys. Fluids*, Vol. 14, No. 2, pp. 744~754.

Mansour, N. N., Kim, J. and Moin, P., 1988, "Reynolds-Stress and Dissipation-Rate Budgets in a Turbulent Channel Flow," *J. Fluid Mech.*, Vol. 194, pp. 15~44.

Moser, R. D., Kim, J. and Mansour, M. M., 1998, "DNS of Turbulent Channel Flow up to Re_τ=590," *Phys. Fluids*, Vol. 11, No. 4, pp. 943~945.

Parneix, S., Laurence, D. and Durbin, P. A., 1998, "A Procedure for Using DNS Databases," *J. Fluids Engrg.*, Vol. 120, pp. 40~47.

Pope, S. B., 1975, "A More General Effective-Viscosity Hypothesis," *J. Fluid Mech.*, Vol. 72, Part 2, pp. 331~340.

Rodi, W., 1976, "A New Algebraic Relation for Calculating the Reynolds Stresses," *Z. Angew. Math. Mech.*, Vol. 56, pp. 219~221.

Smith., G. F., 1971, "On Isotropic Functions of Symmetric Tensors, Skew-Symmetric Tensors and Vectors," *Intl J. Engrg Sci.*, Vol. 9, pp. 899~916.

Spalart, P. R. and Speziale, C. G., 1999, "A Note on Constraints in Turbulence Modelling," *J. Fluid Mech.*, Vol. 391, pp. 373~376.

Speziale, C. G., 1979, "Invariance of Turbulent Closure Models," *Phys. Fluids*, Vol. 22, pp. 1033~1037.

Speziale, C. G. and Gatski, T. B., 1997, "Analysis and Modelling of Anisotropies in the Dissipation Rate of Turbulence," *J. Fluid Mech.*, Vol. 344, pp. 155~180.

Speziale, C. G., Sarkar, S. and Gatski, T. B., 1991, "Modelling the Pressure-Strain Correlation of Turbulence: An Invariant Dynamical Systems Approach," *J. Fluid Mech.*, Vol. 227, pp. 245~272.

Taulbee, D. B., 1992, "An Improved Algebraic Reynolds Stress Model and Corresponding Nonlinear Stress Model," *Phys. Fluid* A, Vol. 4, No. 11, pp. 2555~2561.

Vreman, B., Geurts, B. and Kuerten, H., 1996, "Comparison of Numerical Schemes in Large-Eddy Simulation of the Temporal Mixing Layer," *Int. J. Numer. Meth. Fluids*, 22, pp. 297~311.

Wang, L., 1997, "Frame-Indifferent and Positive-Definite Reynolds Stress-Strain Relation," *J. Fluid Mech.*, Vol. 352, pp. 341~358.

Wallin, S. and Johansson, A. V., 2000, "An Explicit Algebraic Reynolds Stress Model for Incompressible and Compressible Turbulent Flows," *J. Fluid Mech.*, Vol. 403, pp. 89~132.

Wolfram, S., 1988, Mathematica, Addison-wesley.